2120 *Chem. Mater.* **2010,** *22,* 2120–2124
DOI:10.1021/cm902925g

CHEMISTRY OF MATERIALS
Article

High-Performance Solution-Deposited Ambipolar Organic Transistors Based on Terrylene Diimides

Chuan Liu,[†] Zhihong Liu,[§] Henrik T. Lemke,[⊥] Hoi Nok Tsao,[§] Ronald C.G. Naber,[#] Yun Li,[‡] Kulbinder Banger,[†] Klaus Müllen,[§] Martin M. Nielsen,[⊥,∥] and Henning Sirringhaus*,[†]

[†]*Cavendish Laboratory, Madingley Road, Cambridge CB3 0HE, United Kingdom,* [‡]*National Laboratory of Microstructures and Department of Physics, Nanjing University, Nanjing 210093, China,* [§]*Max Planck Institute for Polymer Research Ackermannweg 10, 55128 Mainz, Germany,* [⊥]*Danish National Research Foundation Centre for Molecular Movies, Niels Bohr Institute, University of Copenhagen, Universitetsparken 5, 2100 Copenhagen Ø, Denmark,* [#]*ECN Solar Energy, P.O. Box 1, 1755 ZG Petten, The Netherlands, and* [∥]*Polymer Department, Risø National Laboratory, P.O. Box 49, Frederiksborgvej 399, 4000 Roskilde, Denmark*

Received September 19, 2009. Revised Manuscript Received December 19, 2009

The thin film transistor characteristics of a soluble molecular semiconductor, terrylene tetracarboxdiimide (TDI), a homologue of perylene tetracarboxdiimide (PDI), have been investigated. In a bottom-gate device structure with benzocyclobutene gate dielectric, n-type behavior with electron mobility of 1.1×10^{-2} cm^2 V^{-1} s^{-1} has been observed after thermal annealing. When applied in the top-gate structure with a polycyclohexylethylene-based gate dielectric, TDI devices exhibit ambipolar transport with electron and hole mobility of 7.2×10^{-3} cm^2 V^{-1} s^{-1} and 2.2×10^{-3} cm^2 V^{-1} s^{-1} respectively. The correlation between morphology and field-effect mobility was investigated by atomic force microscopy (AFM) and X-ray diffraction (XRD) studies. Spin-coated, annealed TDI film crystallize in a terrace structure, and the molecules are packed in an "edge-on" structure, thus forming a favorable packing arrangement for charge transport in the plane of the film.

In recent years, significant research efforts have been devoted to searching for organic semiconductor materials for organic field-effect transistor (OFET) applications.[1] High mobility hole transporting semiconducting polymers[2−4] and oligomers[5−9] and electron transporting semiconducting polymers[10−12] and oligomers[13−22] have been developed. Ambipolar materials that simultaneously exhibit hole and electron transport are also attractive, as they enable complementary-like inverters without advanced patterning techniques and new ways to improve the understanding of the physics of these organic devices.[23,24] By choosing a gate dielectric free of electron-trapping groups such as silanol groups, many organic semiconductors that were previously considered to be p-type only became available for n-type transistor fabrication.[10] In this work, we study the application of a soluble oligomer, terrylene tetracarboxdiimide (TDI)[25] (Figure 1, inset), in ambipolar transistors. TDI is the

*Corresponding author. E-mail: hs220@cam.ac.uk.

(1) Sirringhaus, H. *Adv. Mater.* **2005**, *17*, 2411.
(2) Zhang, M.; Tsao, H. N.; Pisula, W.; Yang, C.; Mishra, A. K.; Müllen, K. *J. Am. Chem. Soc.* **2007**, *129*, 3472.
(3) McCulloch, I.; Heeney, M.; Bailey, C.; Genevicius, K.; Macdonald, I.; Shkunov, M.; Sparrowe, D.; Tierney, S.; Wagner, R.; Zhang, W.; Chabinyc, M. L.; Kline, R. J.; McGehee, M. D.; Toney, M. F. *Nat. Mater.* **2006**, *5*, 328.
(4) Ong, B. S.; Wu, Y.; Liu, P.; Gardner, S. *Adv. Mater.* **2005**, *17*, 1141.
(5) Ahmed, E.; Briseno, A. L.; Xia, Y.; Jenekhe, S. A. *J. Am. Chem. Soc.* **2008**, *138*, 1118.
(6) Sun, Y.; Tan, L.; Jiang, S.; Qian, H.; Wang, Z.; Yan, D.; Di, C.; Wang, Y.; Wu, W.; Yu, G.; Yan, S.; Wang, C.; Hu, W.; Liu, Y.; Zhu, D. *J. Am. Chem. Soc.* **2007**, *129*, 1882.
(7) Klauk, H.; Zschieschang, U.; Weitz, R. T.; Meng, H.; Sun, F.; Nunes, G.; Keys, D. E.; Fincher, C. R.; Xiang, Z. *Adv. Mater.* **2007**, *19*, 3882.
(8) Takimiya, K.; Ebata, H.; Sakamoto, K.; Izawa, T.; Otsubo, T.; Kunugi, Y. *J. Am. Chem. Soc.* **2006**, *128*, 12604.
(9) Li, Y.; Wu, Y.; Gardner, S.; Ong, B. S. *Adv. Mater.* **2005**, *17*, 849.
(10) Chua, L. L.; Zamseil, J.; Chang, J.-F.; Ou, E. C. W.; Ho, P. K. H.; Sirringhaus, H.; Friend, R. H. *Nature* **2005**, *434*, 194.
(11) Zhan, X; Tan, Z.; Domercq, B.; An, Z.; Zhang, X.; Barlow, S.; Li, Y.; Zhu, D.; Kippelen, B; Marder, S. R. *J. Am. Chem. Soc.* **2008**, *129*, 7246.
(12) Yan, H.; Chen, Z.; Zheng, Y.; Newman, C.; Quinn, J.; Dötz, F.; Kastler, M.; Facchetti, A. *Nature* **2009**, *457*, 679.
(13) Bao, Z.; Lovinger, A.; Brown, J. *J. Am. Chem. Soc.* **1998**, *120*, 207.
(14) Kobayashi, S.; Takenobu, T.; Mori, S.; Fujiwara, A.; Iwasa, Y. *Appl. Phys. Lett.* **2003**, *82*, 4581.
(15) Jones, B. A.; Ahrens, M. J.; Yoon, M. H.; Facchetti, A.; Marks, T. J.; Wasielewski, M. R. *Angew. Chem., Int. Ed.* **2004**, *43*, 6363.
(16) Song, D.; Wang, H.; Zhu, F.; Yang, J.; Tian, H.; Geng, Y.; Yan, D. *Adv. Mater.* **2008**, *20*, 2142.
(17) Weitz, R. T.; Amsharov, K.; Zschieschang, U.; Villas, E. B.; Goswami, D. K.; Burghard, M.; Dosch, H.; Jansen, M.; Kern, K.; Klauk, H. *J. Am. Chem. Soc.* **2008**, *130*, 4637.
(18) Oh, J. H.; Liu, S.; Bao, Z.; Schmidt, R.; Würthner, F. *Appl. Phys. Lett.* **2007**, *91*, 212107.
(19) Ling, M.-M.; Erk, P.; Gomez, M.; Koenemann, M.; Locklin, J.; Bao, Z. *Adv. Mater.* **2007**, *19*, 1123.
(20) Handa, S.; Miyazaki, E.; Takimiya, K.; Kunugi, Y. *J. Am. Chem. Soc.* **2007**, *129*, 11684.
(21) Yoo, B.; Jones, B. A.; Basu, D.; Fine, D.; Jung, T.; Mohapatra, S.; Facchetti, A.; Dimmler, K.; Wasielewski, M. R.; Marks, T. J.; Dodabalapur, A. *Adv. Mater.* **2007**, *19*, 4028.
(22) Lee, T.-W.; Byun, Y.; Koo, B.-W.; Kang, I.-N.; Lyu, Y.-Y.; Lee, C. H.; Pu, L.; Lee, S. Y. *Adv. Mater.* **2005**, *17*, 2180.
(23) Cornil, J.; Brédas, J.-L.; Zaumseil, J.; Sirringhaus, H. *Adv. Mater.* **2007**, *19*, 1791.
(24) Zaumseil, J.; Sirringhaus, H. *Chem. Rev.* **2007**, *107*, 1296.
(25) Nolde, F.; Pisula, W.; Müller, S.; Kohl, C.; Müllen, K. *Chem. Mater.* **2006**, *18*, 3715.

Published on Web 02/10/2010

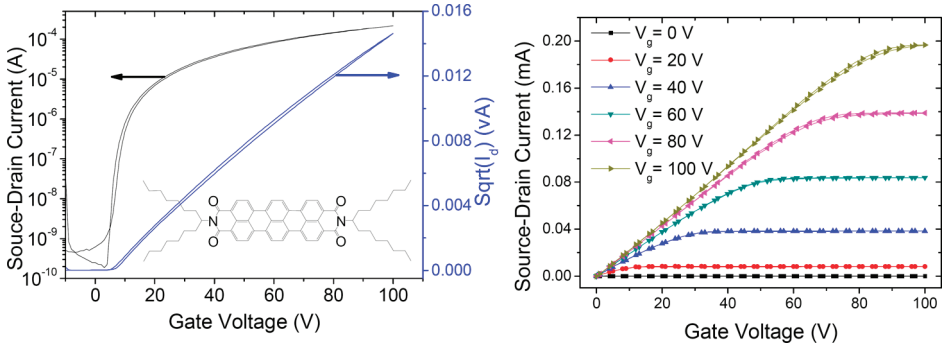

Figure 1. Current−voltage characteristics of bottom-gate, top-contact device with TDI annealed at 180 °C for 10 min (L = 200 μm, W = 10 cm), transfer characteristics and square root of I_d at V_g = 100 V (left), output characteristics (right). I_d, V_d, and V_g represent source-drain current, source-drain voltage, and gate voltage, respectively. Inset: molecular structure of TDI.

higher homologue compound of the liquid crystalline perylene tetracarboxdiimides (PDIs). PDI oligomers exhibit electron mobility up to 10^{-2} cm^2 V^{-1} s^{-1} in FETs,[26] are tunable in terms of their solid-state packing,[15,26−28] and are, therefore, attractive candidates for n-type OFETs. Early study showed that perylene-3,4,9,10-tetracarboxylic-3,4,9,10-dianhydride (PTCDA) can transport holes in the direction normal to the molecular planes in light emitting diodes.[29] Yet it wasn't until recently that another homologue compound of PDI was found to simultaneously exhibit electron and hole mobilities higher than 1×10^{-3} cm^2 V^{-1} s^{-1} in FETs.[30] Here we demonstrate that by using proper device structure and fabrication methods, TDI can be applied in n-channel only devices and can even be made to exhibit high-performance ambipolar behavior.

The synthetic route of TDI has previously been described in detail[25] and the LUMO and HOMO level were measured from solutions via cyclic voltammetry to be 3.5−3.7 eV and 5.2−5.4 eV, respectively. For the bottom gate, top contact FETs, highly doped n-type (100) silicon wafers with 300 nm SiO_2 layers were used as substrates. A thin 60 nm film of benzocyclobutene (BCB)[10] was spun on and cross-linked on top of the SiO_2 to act as a trapping-free interfacial gate dielectric. The TDI thin film was then spin-coated in nitrogen atmosphere from a xylene solution (8 mg/mL) at 1600 rpm for 40 s followed by 4000 rpm for 15 s to produce 30 nm films. Finally, aluminum source-drain electrodes were thermally evaporated through a shadow mask at a rate of 1 Å/s in vacuum of 1×10^{-6} mbar. Channel width (W) and length (L) were 10 cm and 200 μm, respectively. Devices were measured under nitrogen atmosphere with an Agilent 4145B Semiconductor Parameter Analyzer (SPA). Mobilities were extracted from the saturated transfer characteristics.

As-spun films exhibited a low field-effect mobility of 1×10^{-5} cm^2 V^{-1} s^{-1} with large hysteresis. However, after the film was annealed at 180 °C for 10 min, the device performance showed significant enhancement. Figure 1 shows the transfer and output characteristics. When operating with source drain voltage (V_d) of 100 V under nitrogen atmosphere, the annealed sample showed a saturation regime mobility[31] of 1.1×10^{-2} cm^{2}V^{-1}s^{-1}, which is comparable to the highest n-type mobility reported for soluble oligomers.[12,19] The devices have a low turn-on voltage of 3 V and threshold voltage of 5 V, a good subthreshold slope of 1.85 V/decade, and an on/off ratio greater than 1×10^6. Importantly, only minimal hysteresis between backward and forward voltage sweeps is observed. For comparison, we also fabricated bottom gate, bottom contact devices in smaller dimensions (2−20 μm). As BCBs and Al are not easily integrated into a conventional photolithographic process, we used SiO_2 as dielectric and Au as electrodes. The devices still exhibited mobilities up to 8×10^{-3} cm^{2}V^{-1}s^{-1}, and had similarly low turn-on voltage of 2 V and an on/off ratio greater than 10^6 with small hysteresis. The good electron transport in this structure indicates that the electron affinity (E_a) of TDI is sufficiently high such that electron trapping in silanol groups on the surface of the SiO_2 dielectric cannot occur[32] and gold electrodes provide sufficiently good electron injection into the LUMO states of TDI. We note that Au electrodes defined by photolithography have a lower work-function of near 4.7 eV compared to that of atomically clean gold surfaces.[33]

To fabricate top-gate, bottom-contact transistors, we patterned Au source and drain electrodes via photolithography on glass substrates and subsequently deposited and annealed the semiconductor layer using the same conditions as stated above. The gate dielectric layer prepared by depositing 120 nm polycyclohexylethylene (PCHE), 10 nm SiO, and 250 nm poly(vinylidene fluoride-trifluoroethylene) dielectric has previously been shown to be a high-performance top-gate dielectric for ambipolar OTFTs.[34] The samples were annealed at

(26) Chen, Z.; Debije, M. G.; Debaerdemaeker, T.; Osswald, P.; Würthner, F. *ChemPhysChem* **2004**, *5*, 137.
(27) Würthner, F. *Chem. Commun*. **2004**, 1564.
(28) Chen, H. Z.; Ling, M.-M.; Mo, X.; Shi, M. M.; Wang, M.; Bao, Z. *Chem. Mater*. **2007**, *19*, 816.
(29) Ostrick, J. R.; Dodabalapur, A.; Torsi, L; Lovinger, A. J.; Kwock, E. W.; Miller, T. M.; Galvin, M.; Berggren, M.; Katz, H. E. *Appl. Phys. Lett*. **1997**, *81*, 6804.
(30) Tsao, H. N.; Pisula, W.; Liu, Z.; Osikowicz, W.; Salaneck, W. R.; Müllen, K. *Adv. Mater*. **2008**, *20*, 2715.
(31) Here the apparent mobility is used, which includes all the field-dependent series resistances including those near the contacts. Contact resistance was not corrected and so the apparent mobility does not only reflect bulk channel effects.
(32) Singh, T. B.; Meghdadi, F.; Günes, S.; Marjanovic, N.; Horowitz, G.; Sariciftci, N. S. *Adv. Mater*. **2005**, *17*, 2315.
(33) Wan, A.; Hwang, J.; Amy, F.; Kahn, A. *Org. Electron*. **2005**, *6*, 47.
(34) Naber, R. C. G.; Bird, M.; Sirringhaus, H. *Appl. Phys. Lett*. **2008**, *93*, 023301.

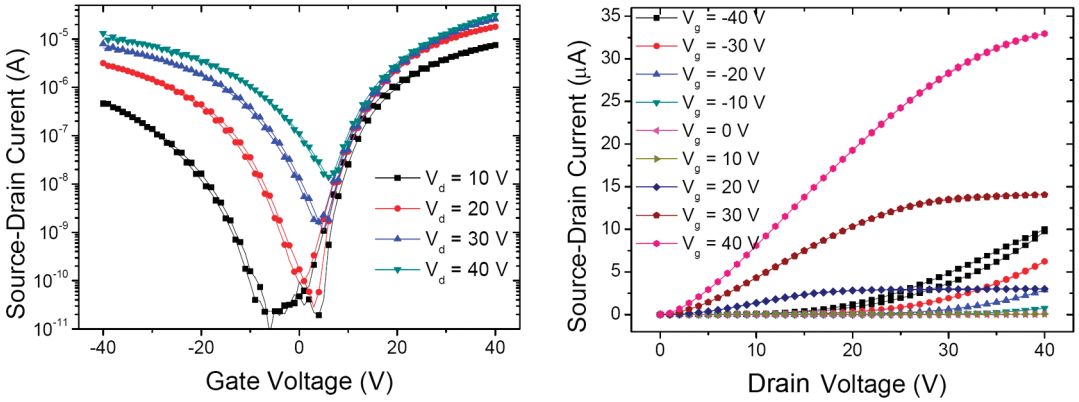

Figure 2. Current−voltage characteristics of top-gate, bottom-contact device with TDI annealed at 180 °C for 10 min before dielectrics were spin coated (L = 20 μm, W = 1 cm, V_d = 40 V), transfer characteristics (left), output characteristics (right).

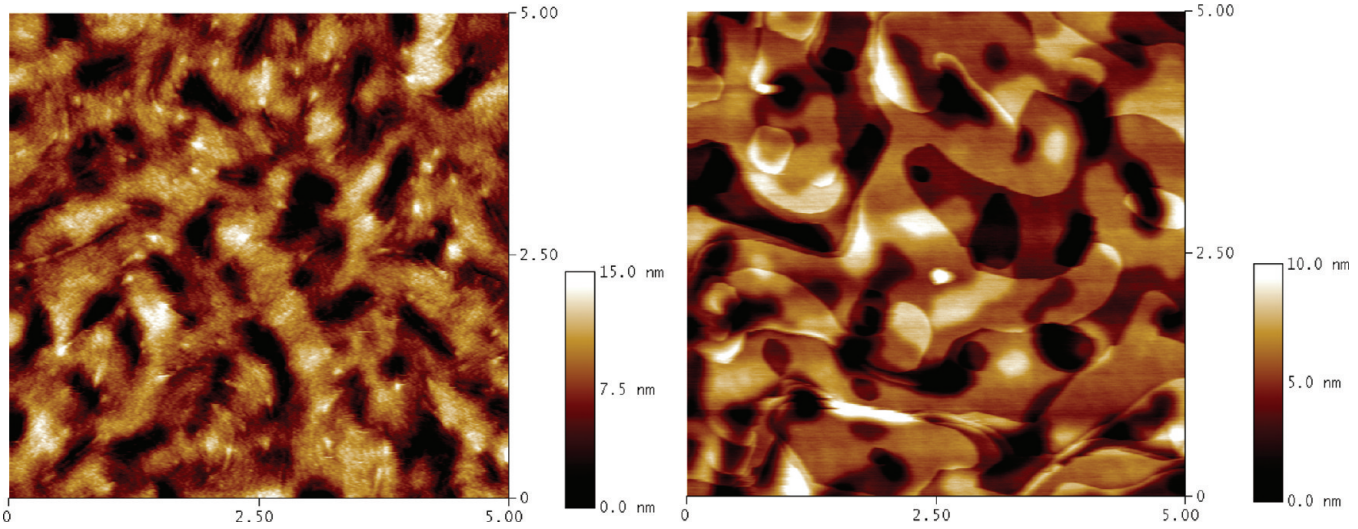

Figure 3. Tapping mode AFM image of TDI film, topographic image of as-spun film (left), film annealed at 180 °C for 10 min (right). Average surface roughness of the areas taken was 27.8 and 18.0 nm, respectively.

120 °C for 1 h after the deposition of the dielectric layer and finally Au gate electrodes were evaporated on top through a shadow mask. The transfer and output characteristics of a 20 μm long and 1 cm wide device are shown in Figure 2. In contrast to the bottom-gate structure the top-gate device exhibited clean ambipolar characteristics with small hysteresis. The extracted n-type mobility was 7.2×10^{-3} cm^2 V^{-1} s^{-1} and the p-type mobility was 2.2×10^{-3} cm^2 V^{-1} s^{-1} in the saturation regime. To the best of our knowledge, ambipolar behavior has not been reported in a PDI derivative before, although similar ambipolar characteristics have recently been observed in quaterrylene tetracarboxdiimide (QDI).[30] This is most likely due to the HOMO level of the higher homologues of PDI being more easily accessible for charge injection from gold electrodes. We were unable to investigate light emission from the TDI devices because of the emission occurring in the infrared around 770 nm where our CCD camera is not sufficiently sensitive.[35]

We currently do not understand well the reasons why we cannot also observe ambipolar behavior in the bottom-gate device configuration. This could possibly be due to a contact resistance effect for hole injection into the HOMO of TDI. In the top-gate, staggered structure, the contact resistance tends to be smaller than in the coplanar bottom-gate, bottom-contact structure because of current crowding effects and in the staggered bottom-gate, top-contact structure where metal interdiffusion occurring during evaporation of the contacts can be an issue.[36,37] Alternatively, the effect could be due to hole trapping in states at the TDI/BCB/SiO_2 interface or due to specific molecular packing geometries at the bottom interface of the film that constitute charge traps for holes in the HOMO, but not electrons in the LUMO. We note that the ambipolar behavior observed in our TDI films is qualitatively different from that reported for QDI devices. In the latter, ambipolar behavior was observed only in as-deposited bottom-gate devices, whereas hole transport disappeared after film annealing at 100 °C.[30] In our bottom-gate TDI devices, we cannot detect any hole transport even in the as-deposited films, but the mobility of the as-deposited TDI films is generally much lower

(35) Zaumseil, J.; Donley, C. L.; Kim, J.-S.; Friend, R. H.; Sirringhaus, H. *Adv. Mater.* **2006**, *18*, 2708.
(36) Richards, T.; Sirringhaus, H. *Appl. Phys. Lett.* **2008**, *92*, 023512.
(37) Richards, T.; Sirringhaus, H. *J. Appl. Phys.* **2007**, *102*, 094510.

than that of as-deposited QDI films. In our top-gate TDI devices, both electron and hole mobilities were clearly found to improve upon annealing.

To investigate the cause for the improvement of mobility by 3 orders of magnitude upon annealing, film morphology and microstructure were studied. Under a cross-polarized microscope equipped with UV excitation, the as-spun films appeared amorphous, whereas the films annealed at 180 °C showed polycrystalline domains with size of tens of micrometers. After higher temperature annealing at 330 °C, the grain size increased to up to 100 μm but the device performance dropped compared to films annealed at 180 °C because of film dewetting. In atomic force microscopy (AFM), the as-spun film exhibited a fibrillar surface morphology but no clear evidence of crystalline order (Figure 3, left). Films annealed at 180 °C had a crystalline structure with well-defined surface steps with a height of around 2−3 nm (Figure 3, right) separating large, molecularly flat terraces with little roughness. However, some of the terraces exhibited smooth variations in surface topography with protrusions of up to 5 nm (white areas, in Figure 3, right), which indicates the existence of subsurface defects.

To further assess the thin film microstructure of TDI, X-ray diffraction (XRD) experiments were performed on both as-spun and annealed films. The $\theta/2\theta$ scans of the annealed films indicate a significantly textured thin film microstructure. From the 001 reflections, interlayer spacing of 24.9 Å perpendicular to the substrate surface can be determined (data not shown here), which is corresponding to the smallest surface step height (~2 nm) observed in AFM. In contrast to the annealed films, the as-spun films showed much weaker diffraction peaks, suggesting amorphous or low crystallinity of the films.

Two-dimensional grazing incidence wide-angle X-ray scattering (GIWAXS) patterns of a spin coated thin film are shown in Figure 4 before and after being annealed to 180 °C. The GIXD data were recorded using a rotating anode based diffractometer at Risø National Laboratory, Roskilde.[38] The wavelength λ was 1.5418 Å (CuKα), monochromated by a multilayer X-ray mirror. The X-ray incidence angle with respect to the sample plane was at 0.18° (just below the critical angle of Si (also SiO_2)). The X-ray diffraction signal was recorded on a Fuji image plate. The signal from the as-spun film (Figure 4a) indicates a columnar "edge-on" phase by a columnar diffraction peak, and an entirely in-plane reflection at $Q_{\|} = 1.7$ Å^{-1} which can be attributed to a typical π-stacking distance of 3.7 Å. Q is the (3D) reciprocal space vector, its length, represents a real-space periodicity $d = 2\pi/|Q|$. $Q_{\|}$ and $Q_{\perp}$ are its components parallel and perpendicular to the sample plane. The alignment distribution can be determined from the azimuthal broadening of the columnar reflection. The azimuthal angle χ, (defined as $\tan(\chi) = Q_{\perp}/Q_{\|}$) of the columnar reflection (22.8° ≠ 30°) suggests an orthorhombic packing of TDI columns rather than a hexagonal packing. When identifying the columnar reflections as the 110 reflection, the packing distances become $a = 2.8$ nm and $b = 6.6$ nm.

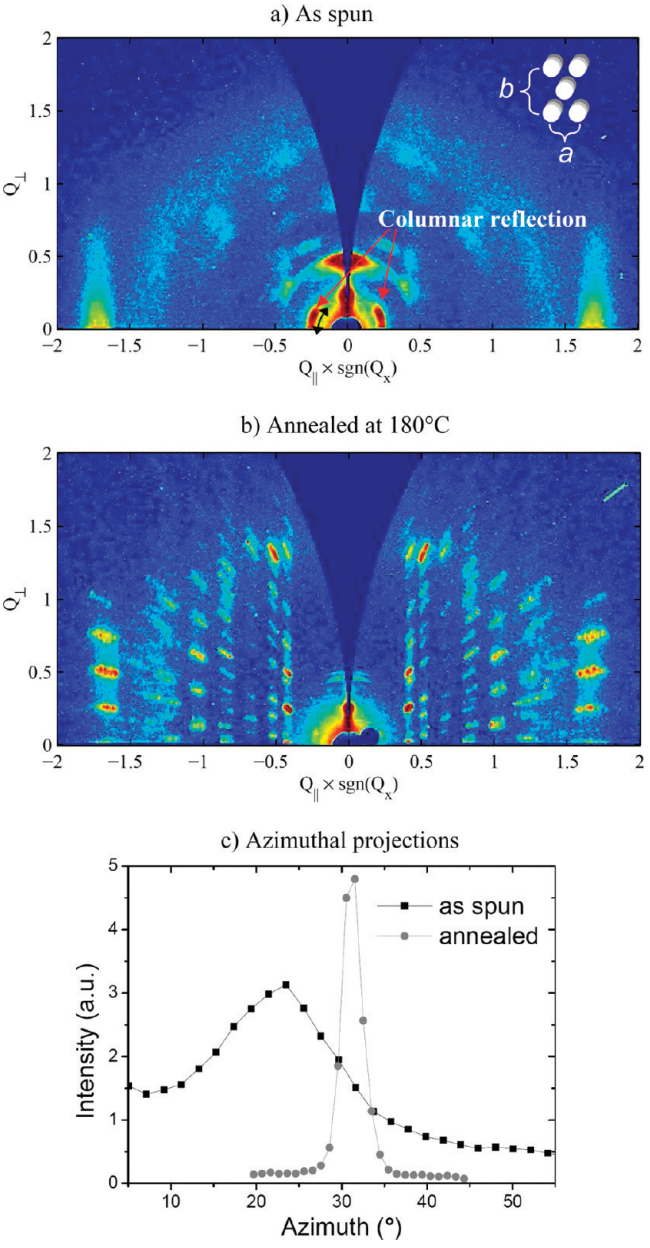

Figure 4. XRD patterns of a TDI film on SiO_2 (a) before and (b) after annealing at 180 °C. The data were transformed from detector space to rotational symmetric coordinates of the wave vector transfer Q. The sgn(Q_x) is added in order to indicate the two half spaces which show identical behavior due to the rotational symmetry. Units are Å^{-1} for X and Y axis. The inset in a shows a possible packing of columns. In a, the azimuthal direction used for extracting the peak profiles is indicated by a black double-arrow. (c) Azimuthal projections of the columnar reflections in a and b. The reflections of the "as-spun" and annealed film are centered at 22.8° and 31.1° with a full width at a half-maximum of 13.4° and 2.7°, respectively (determined by Gaussian fits).

When annealing the spin-coated films to 180 °C and cooling them back to room temperature, a transition to a crystalline phase with a high degree of long-range order occurs (Figure 4b). This is indicated by well-defined Bragg reflections up to a high Q. The alignment distribution with respect to the substrate plane determined from the azimuthal width of the strong reflection at

(38) Apitz, D.; Bertram, R. P.; Benter, N.; Hieringer, W.; Andreasen, J. W.; Nielsen, M. M.; Johansen, P. M.; Buse, K. *Phys. Rev. E* **2005**, *72*, 036610.

$(Q_{\parallel},Q_{\perp}) = (0.42,0.25)$ Å^{-1} (2.7° fwhm) is much higher than in the "as-spun" case. This reflection gives rise to a 1.5 nm periodicity in the in-plane direction and a 2.51 nm out-of-plane periodicity. This asymmetry of in-plane and out-of plane periodicity qualitatively agrees with the elongated shape of the TDI molecule and points toward a parallel "edge-on" packing with the long molecular axis in the out-of-plane direction instead of a helical packing which would result in a higher symmetry of the column. Both types of packing were proposed by Nolde et al.[25] Strongly weighted in-plane reflections at $Q_{\parallel} = 1.7$ Å^{-1}, representing a π-stacking distance of 3.7 Å within the columns, support the edge-on packing. However, the exact crystal symmetry and the unit-cell parameters remain unsolved.

The XRD measurements provide an explanation for the large improvement in device performance observed upon annealing. The low mobility in as-spun devices corresponds to an "edge-on", orthorhombic columnar phase in the microstructure in which the side chains of he TDI molecules are oriented either out-of-plane or in-plane, potentially in a helical arrangement. In these charge transport tends to be one-dimensional along the columns and is frequently impeded by the long alkyl side chains, when charge carriers need to hop from one column to the neighboring one. The much higher mobility in the annealed devices corresponds to an also "edge-on" but crystalline phase, in which the long axis and the side chains of the TDI molecules are preferentially oriented perpendicular to the substrate. In this case in-plane charge transport is likely to be more two-dimensional in layers of more closely packed TDI molecules. Further enhancement of mobility might be obtained through further optimization of the film microstructure.

In summary, we have demonstrated that terrylene tetracarboxdiimide (TDI) is a suitable material for fabricating high performance thin film transistors with solution processing methods. TDI shows clean n-type operation in bottom-gate devices and ambipolar operation in top-gate, staggered devices. TDI is potentially a useful n-type semiconductor for application to CMOS organic circuits. With further optimization of molecular structure, such as substitution of electron withdrawing groups in the bay region to increase the electron affinity and optimization of side chain substitution to improve molecular packing similar to the optimization undertaken for PDI,[39,40] even higher levels of performance may be achievable.

Acknowledgment. H.T.L. thanks Jens Wenzel Andreasen (Technical University of Denmark, Risø, Denmark) for kind assistance acquiring the X-ray data as well as the Danish National Science Foundation's Centre for Molecular Movies for funding.

(39) Jones, B. A.; Facchetti, A.; Wasielewski, M. R.; Marks, T. J. *J. Am. Chem. Soc.* **2007**, *129*, 15259.
(40) Schmidt, R.; Oh, J. H.; Sun, Y.-S.; Deppisch, M.; Krause, A.-M.; Radacki, K.; Braunschweig, H.; Könemann, M.; Erk, P.; Bao, Z.; Würthner, F. *J. Am. Chem. Soc.* **2009**, *131*, 6215.